

A Microelectrode Modified with Co-electrodeposited Carboxyl Graphene and AuNPs: Characterization and Application in Water Quality Detection

Yijin Li^{1,*}, Jizhou Sun², Jinfen Wang³, Shanhong Xia²

¹ School of Mechanical Electronic and Information Engineering, China University of Mining & Technology, Beijing, China

² State Key Laboratory of Transducer Technology, Institute of Electronics, Chinese Academy of Sciences, Beijing, China

³ CAS Center for Excellence in Nanoscience, National Center for Nanoscience and Technology, Beijing, China

*E-mail: Kathy_91@163.com

Received: 3 August 2018 / *Accepted:* 29 September 2018 / *Published:* 5 November 2018

A microelectrode modified with carboxyl graphene and Au nanoparticles (AuNPs) was developed, and the application of the microelectrode in water quality detection was studied. The microelectrode was fabricated by Micro-Electro-Mechanical System (MEMS) techniques to accurately control the shape and the dimensions. Carboxyl graphene and AuNPs were co-electrodeposited on the microelectrode through chronoamperometry. Scanning electron microscope (SEM), cyclic voltammetry (CV), electrochemical impedance spectroscopy (EIS) and Raman spectroscopy were employed to investigate the modification process. The co-electrodeposited microelectrode displays better conductivity and more uniform distribution than individually modified electrodes due to the synergistic interaction of carboxyl graphene and AuNPs. By combining the advantages of co-electrodeposition and microelectrodes, sensitive and rapid detection can be achieved. The modified electrode showed a sensitivity of $-75.23 \text{ nA} \cdot (\text{mg/L})^{-1}$ for dissolved oxygen detection, which is approximately five times that of a bare electrode. The carboxyl functional groups on deposited carboxyl graphene can provide immobilization sites for subsequent biochemical materials, which extends the application of the modified electrode. As an example, by further immobilization of microorganisms, the modified electrode offered a fast detection method for biochemical oxygen demand. The proposed modified electrode is promising for rapid and sensitive water quality detection.

Keywords: Co-electrodeposition; carboxyl graphene; Au nanoparticles; sensitive and fast detection

1. INTRODUCTION

Since water pollution is serious in many regions, the acquisition of water quality data has become more and more important for early warning, pollution control and the setup of environmental monitoring systems [1,2]. Aiming at different water quality parameters, various methods including national standard methods and industrial standard methods have been recommended to obtain accurate measurement results. However, most of the methods are laboratory techniques, requiring complicated sample preparation, expensive instruments and chemical reagents, a long detection time and practiced operation. Thus, water quality monitoring calls for sensitive, rapid and easy-to-operate detection methods to satisfy the increasing detection requirements.

One of the most important water quality monitoring parameters is dissolved oxygen (DO). The survival of aquatic plants and creatures relies on the proper content of DO. Many chemical and biochemical reactions are directly or indirectly influenced by the content of DO [3]. The DO change caused by microbial biochemical reactions in water is defined as biochemical oxygen demand (BOD), which is also an important parameter for characterizing the self-cleaning ability of water. The traditional methods for DO and BOD detection are iodometry and 5-day BOD (BOD₅), respectively. These methods need complicated procedures and operations, which are time consuming. Thus, sensors for rapid and sensitive detection are preferred [4].

Electrochemical methods, characterized by a short analytical time, high sensitivity and easy adaptability for in situ measurement, have attracted much attention in the field of detection [5]. However, electrochemical detection methods using a bare electrode have a limited application due to the bare electrode's low selectivity, low sensitivity and long response time. By electrode modification, the detection performance can be obviously improved. Thus, with the utilization of new materials and new synthesis methods, electrode modification is one of the most popular areas of research [6-8].

Graphene (GN) has exhibited several excellent properties in terms of fast electron mobility, large theoretical surface area, high current density, superior electrical conductance, high mechanical strength, etc. [9,10]. These properties make graphene very suitable for developing sensors and biosensors with high sensitivity and short response time [11-13]. Individually or as graphene composites, graphene has been widely used in electrode modification to improve detection properties [12,14]. An easy and commonly used method for graphene's electrode modification is the drop-casting method [15,16]. However, graphene modified by this method is not stable enough and is not appropriate for microelectrodes. Another method for graphene modification is the reduction of graphene oxide (GO). There are three fundamental reduction methods, including thermal reduction, chemical reduction and electrochemical reduction [17]. Unlike thermal reduction's damage to structure and chemical reduction's utilization of toxic reagents, electrochemical reduction is considered to be a green reduction method. Electrochemical reduction is efficient, rapid and inexpensive and can also maintain the electronic properties and the electrochemical properties of graphene [18]. Further, the rough surface formed by electrochemical reduction can facilitate the diffusion of electrolyte ions and expose more active sites [19], which can help to increase sensor response and biosensor immobilization sites. However, graphene tends to aggregate readily during the preparation process. To avoid the aggregation of graphene nanosheets during electrodeposition, Au nanoparticles (AuNPs) can

be intercalated [20]. AuNPs are also an excellent type of nanomaterial for fabricating electrochemical sensors and biosensors because of their good conductivity, large surface-to-volume ratio, high catalysis activity and biocompatibility [21,22].

In this paper, carboxyl graphene (GN-COOH) and AuNPs were co-electrodeposited on microelectrodes to fabricate a sensitive interface. The modification process was investigated and the characterization of the interface was studied by scanning electron microscope (SEM), cyclic voltammetry (CV), electrochemical impedance spectroscopy (EIS) and Raman spectroscopy. To confirm the superiority of the modified electrode in detection time, sensitivity and potential in further immobilization, dissolved oxygen and biochemical oxygen demand were detected.

2. MATERIALS AND METHODS

2.1. Reagents and Apparatus

GN-COOH (carboxyl ratio >5.0 wt. %) was obtained from Nanjing XFNANO Materials Tech Co., China. Gold (III) chloride trihydrate ($\text{HAuCl}_4 \cdot 3\text{H}_2\text{O}$, Au%>48%) was purchased from Sigma-Aldrich. AZ1500 and SU-8 were purchased from AZ Electronic Materials and MicroChem Corp Company, respectively. *Bacillus subtilis* (*B. subtilis*) was obtained from the Institute of Microbiology, Chinese Academy of Sciences. All other chemicals were of analytical grade and were used without further purification. Deionized water with a resistivity of 18 M Ω was used throughout the experiments. Phosphate buffer solutions (PBS, 5 mM, pH 7.0) were prepared by mixing KH_2PO_4 , Na_2HPO_4 and 0.1 M NaCl. Different DO solutions were obtained by dissolving Na_2SO_3 in PBS. The DO concentrations of the prepared solutions were detected by a commercial DO meter (Eutech CyberScan DO110 Dissolved Oxygen Meter, Vernon Hills, IL, USA). BOD standard solutions were prepared with glucose and glutamic acid dissolved in PBS.

A three-electrode system containing a modified Au disk microelectrode as the working electrode, a Au ring counter electrode and a commercial saturated Ag/AgCl electrode as the reference electrode (CRE) was constructed for electrochemical measurements. Electrochemical experiments were carried out with a Gamry Reference 600 electrochemical measurement system (Gamry Instruments Co., Ltd., USA). SEM analysis was carried out on a S-4800 field emission scanning electron microscope produced by Hitachi (Tokyo, Japan). Raman spectra were obtained on an AvaRaman-532TEC (AVANTES B.V., Eerbeek, Holland) employing a 532 nm laser beam.

2.2 Microelectrode fabrication

The fabrication process is schematically shown in Fig. 1. The microelectrode was fabricated by standard photolithographic, sputtering and lift-off techniques. A layer of Au (2000 Å), together with an adherent layer of Ta (300 Å), was first sputtered onto a glass wafer. After photolithography and lift-off, the negative photoresist (SU-8) was used to accurately confine the size of the electrodes and act as an insulating layer. The area of the working electrode was 1 mm². By cutting the patterned glass into

individual chips, wire-bonding and encapsulating on a printed circuit board, the microelectrode could be used for subsequent modification and electrochemical detection.

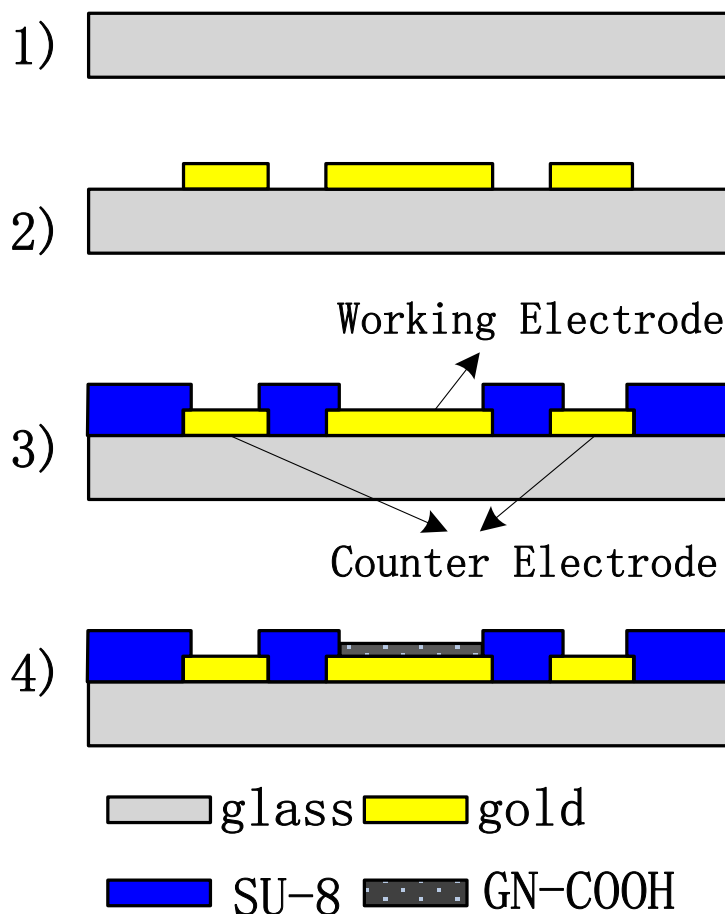


Figure 1. The fabrication process of the microelectrode

2.3 Microelectrode Modification

To completely clean the microelectrode, two steps were taken. First, the microelectrode was treated by oxygen plasma etching with 50 W power for 3 min. The second step was cyclic voltammetric scanning in 5 mM H_2SO_4 until a reproducible voltammogram was obtained. The electrodeposition of GN-COOH was performed in an electrolyte containing 2 mg/ml GN-COOH, 0.1 M LiClO_4 , 0.073 mM HAuCl_4 and 5 mM PBS with N_2 bubbling. PBS was used as a supporting electrolyte, which guaranteed the stability and the effectiveness of the electrodeposition [23]. HAuCl_4 was used to be reduced to AuNPs, which can avoid the aggregation of the electrodeposited GN-COOH. The electrodeposition included two procedures. To increase the activity of the electrode surface, chronoamperometry at -0.6 V for 100 s was first performed for AuNPs deposition. Then, GN-COOH and AuNPs were simultaneously electrodeposited by chronoamperometry at -1 V for 330 s. The modified electrode was washed with deionized water and dried in the air. For comparison,

electrodeposition was also performed in electrolyte without HAuCl_4 or without GN-COOH.

Before DO detection, electrochemical reduction performed by cyclic voltammetry from 0 to -1.1 V for 10 cycles in N_2 -saturated PBS was done to further improve conductivity. Before BOD detection, cells of *B. subtilis* were immobilized onto the modified electrode by sequential carboxyl activation (with EDC and NHS) and cell suspension dropping (20 μl), which has been illustrated in our former work [24]. After immobilization, conductivity was enhanced by the same method as before DO detection.

2.4 Measurement Procedures

The characterization of the electrodeposition process was carried out by CV in different electrolytes in the range from 0 to -1.3 V at 50 mV/s. CV measurements of the modified microelectrode were carried out in 0.1 M KCl containing 2 mM $\text{K}_3[\text{Fe}(\text{CN})_6]$ as a redox probe. The potential range was from -0.2 V to 0.6 V. EIS measurements of the modified microelectrode were conducted in 0.1 M KCl containing 20 mM $\text{K}_3[\text{Fe}(\text{CN})_6]$. The alternative potential was 5 mV, the formal potential was 260 mV and the frequency range was $10^5 - 0.1$ Hz. The DO measurements were carried out by linear scan voltammetry in the range of 0 V to -0.8 V. The currents obtained at -0.5 V were recorded as the current responses. BOD was detected by the chronoamperometry method at a potential of -0.5 V (vs CRE). The difference value between the stable response in PBS and the third minute's response in BOD solution was calculated as the BOD response to this BOD concentration.

3. RESULTS AND DISCUSSION

3.1 The synergistic effect of co-electrodeposition

Fig. 2A displays the comparison between the CV responses of the electrodeposition process in three different electrolytes. The CV of the microelectrode immersed in the electrolyte containing only GN-COOH (a) shows an obvious reduction peak at around -1.0 V, which indicates the reduction of carboxyl groups on electrode surface. The GN-COOH has been reduced electrochemically at negative potentials quickly and irreversibly. The CV curve obtained in the electrolyte containing only HAuCl_4 (b) is shown in Fig. 2A(b).

Two reductive peaks can be seen at approximately -0.77 V and -1.15 V, owing to the reductive behaviour of HAuCl_4 to AuNPs. When the microelectrode is immersed in the electrolyte containing both GN-COOH and HAuCl_4 , the CV curve (c) shows two remarkable reduction current peaks at -0.7 V and -1.08 V. In addition, the reduction currents obtained in the mixture are much larger than those obtained in each of the electrolytes.

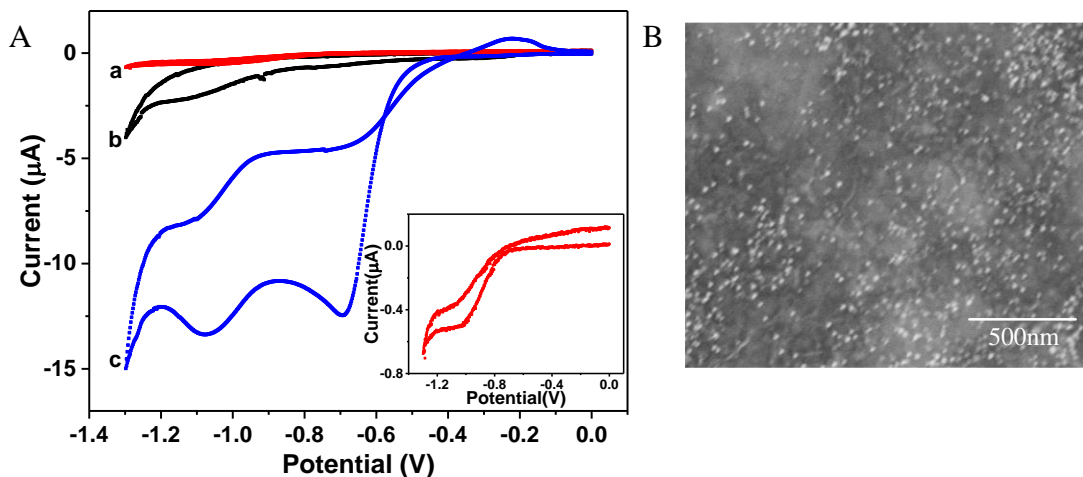


Figure 2. (A) CV curves of the Au microelectrode in an aqueous solution of (a) 2 mg/ml GN-COOH, (b) 0.073 mM HAuCl₄, and (c) 2 mg/ml GN-COOH + 0.073 mM HAuCl₄. (B) SEM image of the co-electrodeposited surface.

The electrodeposition CV curves retain a similar shape to those in related studies [25,26]. These results indicate that the conductivity becomes much higher after the co-electrodeposition of GN-COOH and HAuCl₄. Thus, the synergistic effect of electrodeposited GN-COOH and AuNPs has been illustrated, which can further improve the conductivity of the modified microelectrode.

The surface morphology characterized by SEM is shown in Fig. 2B. A coarse and crumpled surface is observed. The GN-COOH is layer-packed, and many AuNPs are dispersed in the electrodeposited GN-COOH. However, the boundaries of the AuNPs are not clear enough. This can be explained by the intercalation of AuNPs in the electrodeposited GN-COOH. The intercalation of AuNPs can avoid the aggregation of GN-COOH, leading to improved conductivity and increased surface area, which are suitable for electrochemical sensing.

3.2 Characterization of the modified electrode

CV provides an effective method for characterizing the interface surface properties of modified electrodes. Ferricyanide is a widely used probe in CV scanning owing to its excellent oxidation-reduction performance.

Fig. 3A shows the CV curves of modified electrodes after electrodeposition in different electrolytes. A pair of well-defined redox peaks are obtained on a bare Au microelectrode (a), representing the reversible electron transfer between [Fe(CN)₆]³⁻ and the microelectrode. After the electrodeposition in HAuCl₄, the modified electrode displays smaller CV peak currents (b) compared with the unmodified electrode.

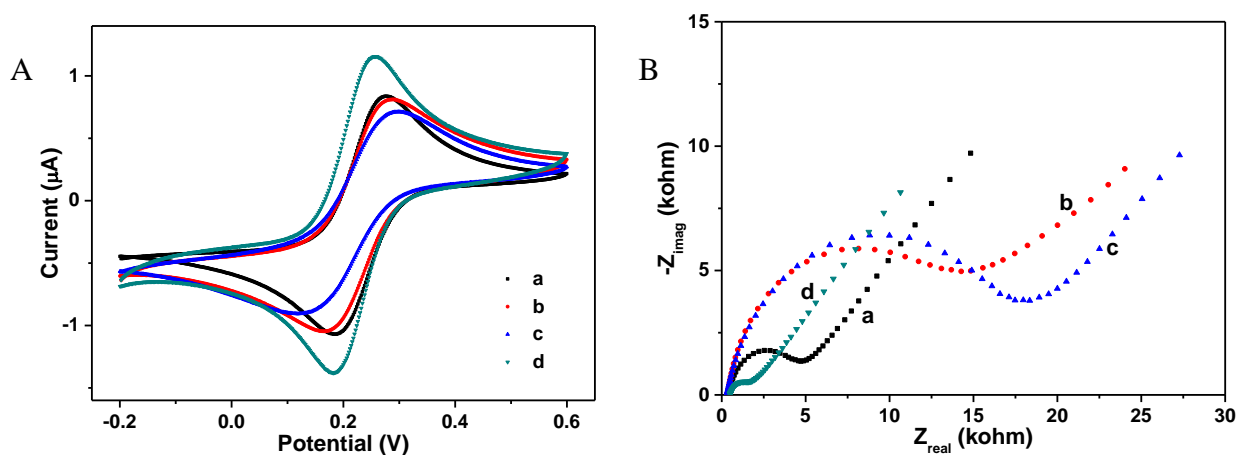


Figure 3. CV curves (A) and EIS curves (B) of different modified microelectrodes in 2 mM (A) and 20 mM (B) $K_3Fe(CN)_6$ solutions. The microelectrodes were electrodeposited in electrolytes containing no additive (a), $HAuCl_4$ (b), GN-COOH (c) and $HAuCl_4 + GN-COOH$ (d).

This indicates that the electrodeposition of $HAuCl_4$ only is not efficient because of the low concentration. When electrodeposition is carried out in the solution containing GN-COOH, the modified electrode also provides small CV peak currents (c). This suggests that aggregation occurs on the modification surface and that the reduction of GN-COOH is not sufficient. Interestingly, when the electrode is modified by the co-electrodeposition of GN-COOH and AuNPs, the CV curves obtained in ferricyanide solution show a remarkable increase in peak currents. The conductivity of the modified electrode is also improved. This indicates that both GN-COOH and AuNPs have been deposited onto the electrode surface. The deposition of the two nano-materials is mutually facilitated, which is in accordance with our conclusion obtained from Fig. 2A.

EIS is another useful technique for studying electron transfer characterizations of the modified electrodes. The semicircle diameter in the impedance spectrum represents the electron transfer resistance. The bigger the semicircle diameter is, the larger the electron transfer resistance is. Fig. 3B displays the EIS curves of different modified electrodes. As seen from curve a, the unmodified electrode shows a standard EIS semicircle profile, indicating good electrochemical electrode characterization. After electrodeposition of AuNPs or GN-COOH, the modified electrodes offer larger semicircle diameters (curves b and c) compared with the unmodified electrode. The changes in electron transfer resistance suggest that AuNPs and GN-COOH have been electrodeposited onto the electrode surface respectively and that the electrodepositions lower the electrodes' electron transfer capability. The result can be attributed to the low concentration of $HAuCl_4$ and insufficient reduction of GN-COOH. However, when AuNPs and GN-COOH are co-electrodeposited while the other experimental conditions remain the same, the modified electrode shows an obvious decrease in semicircle diameter and electron transfer resistance (curve d). This can be explained by the synergistic effect of AuNPs and GN-COOH. The intercalation of AuNPs in layered GN-COOH improves the electrodeposition structure and morphology, which in turn improves conductivity and the electrodes' electrochemical performance.

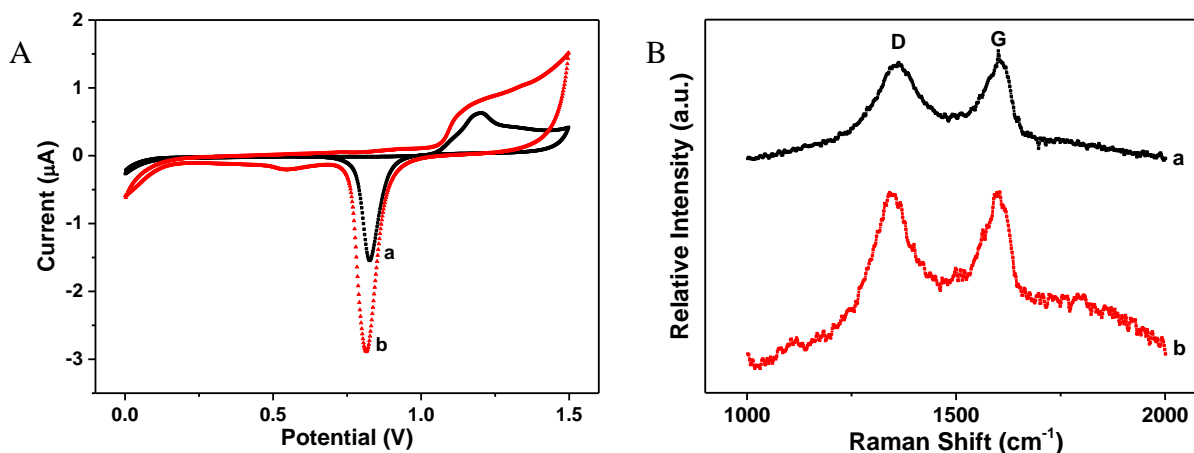


Figure 4. (A) CV curves of bare Au (a) and GN-COOH-AuNPs/Au (b) in 5 mM H₂SO₄; (B) Raman spectra of GN-COOH (a) and electrodeposited GN-COOH (b).

The electrodeposition status of AuNPs can be characterized by CV scanning in H₂SO₄ solution. The reduction peak of Au oxide in H₂SO₄ solution can be used to represent the surface area of Au electrode. Fig. 4A reveals the electrodes' CV curves in 5 mM H₂SO₄. An obvious reduction peak at 0.82 V is obtained on the bare Au electrode (curve a). After the deposition by chronoamperometry at -1.0 V for 330 s, an apparent increase in reduction peak current is observed (curve b). This indicates that H₂AuCl₄ is reduced to AuNPs and that AuNPs are immobilized onto the electrode, adding the active electrode area and conductivity.

Raman spectroscopy can provide information about the structure of carbon clusters and is proven to be an effective method for the characterization of GN materials. As seen in Fig. 4B, the Raman spectra of GN-COOH exhibit two quite sharp bands. The D bands at 1350 cm⁻¹ correspond to sp³-hybridized carbons, representing the presence of disordered structures in the GN material. The G bands at 1601 cm⁻¹ correspond to the E_{2g} zone center mode of crystalline graphite, representing ordered structures in the GN material. The intensity ratio of the D and G bands (I_D/I_G) is in direct proportion to the number of defect sites [27]. After electrodeposition, the I_D/I_G ratio increases from 0.89 to 1.00. This suggests that more defect sites are formed due to the reduction of GN-COOH and the intercalation of AuNPs.

3.3 Sensitive response to DO

The electrocatalytic properties of GN-COOH-AuNPs/Au for DO detection were investigated. Fig. 5A displays the linear scan voltammograms in oxygen-removed PBS (a and b) and air-saturated PBS (c and d), respectively. Compared with bare Au electrode (a and c), GN-COOH-AuNPs/Au electrode (b and d) shows a more positive electroreduction potential (from -0.15 V) and larger reduction current (522.8 nA at the potential of -0.5 V). This indicates the good electrocatalysis performance of the electrodeposited film to DO owing to the utilization of functionalized graphene and AuNPs [28,29].

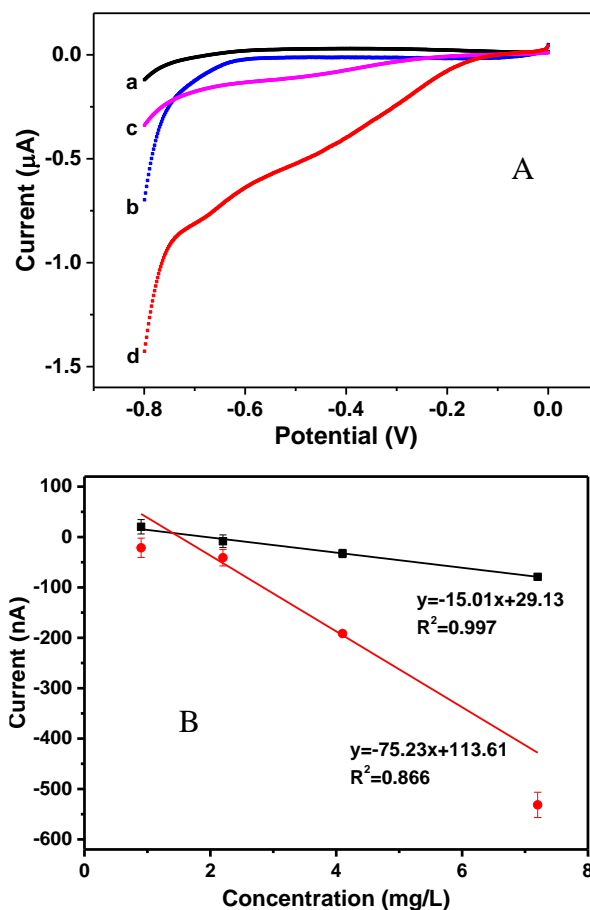


Figure 5. (A) Response of the bare microelectrode in oxygen-removed PBS (a) and air-saturated PBS (c), and the response of the modified microelectrode in oxygen-removed PBS (b) and air-saturated PBS (d); (B) The calibration curve of the bare electrode (black) and modified electrode (red).

The DO measurements were carried out by linear scan voltammetry in the range of 0 V to -0.8 V. The currents obtained at -0.5 V were recorded as the current responses. The current responses to different concentrations of DO solutions were detected, and the calibration curves are shown in Fig. 5B. The current responses decrease linearly with the increase in DO concentration from 0.9 to 7.2 mg/L. The linear equation is $y = -75.23x + 113.61$. The sensitivity of the modified microelectrode is $-75.23 \text{ nA} \cdot (\text{mg/L})^{-1}$, which is approximately five times that of the bare microelectrode. Thus, the use of this modified electrode in sensitive DO detection is promising.

3.4 BOD response of the proposed electrode with further immobilization of microorganisms

The deposition of carboxyl graphene on the modified microelectrode can not only improve the electrode's performance, but also offer carboxyl functional groups for further immobilization of biochemical materials, which can greatly extend the range of applications. By utilizing the carboxyl groups of GN-COOH, microorganisms with amino groups on their surface can be immobilized onto the modified electrode through covalent bonding of carboxyl and amino groups. Thus, BOD can be

measured with this further modified electrode. After immobilizing microorganisms, the electron transfer resistance clearly increases compared with that of the unmodified electrode and the GN-COOH-AuNPs/Au electrode. This suggests that non-conducting microorganisms are successfully immobilized onto the electrode.

By using the proposed electrode for detection, the response time was tested. As seen from Fig. 6A, the current clearly decreased at the beginning, then became stable at the third minute. Thus, the response time to BOD was shortened to 3 min, which was rapid compared with the results of other research [30-32]. The modified electrode was used for rapid BOD detection, and the calibration curve is shown in Fig. 6B. A linear current response is obtained in the BOD concentration range from 2 to 15 mg/L. The linear equation is $y=3.71x-1.48$, with a correlation coefficient of 0.990.

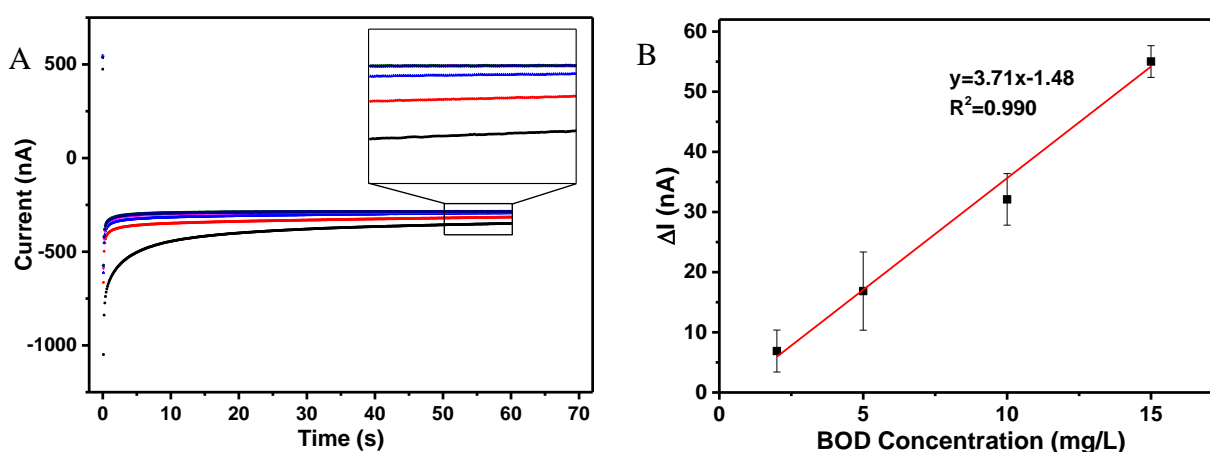


Figure 6. (A) Current response of the *B. subtilis*-modified electrode to 15 mg/l BOD solution in the first five minutes of contact (curves from bottom to top correspond to 0 min to 5 min). Inset is the magnification of each response at 50 to 60 s; (B) The calibration curve of the modified electrode with BOD solutions.

4. CONCLUSIONS

Graphene has unique properties in electrochemical sensing. Based on graphene's good electrochemical activity and its functionalization with carboxyl for electrodeposition, a microelectrode modified with co-electrodeposited GN-COOH and AuNPs has been developed. Compared with electrodes modified with either GN-COOH or AuNPs, the co-electrodeposited modified electrode displays a higher deposition efficiency, better conductivity and larger surface area. When applied to DO detection, catalysis is observed, and good sensitivity is obtained. In addition, the carboxyl graphene can extend the application range of the modified electrode owing to the presence of carboxyl groups as immobilization sites for further biochemical materials' immobilization. By utilizing the carboxyl functional groups of GN-COOH, microorganisms can be immobilized onto the modified electrode through covalent bonding, and BOD can be rapidly detected. Thus, the microelectrode

modified with co-electrodeposited GN-COOH and AuNPs is promising in electrode modification and water quality sensing.

ACKNOWLEDGMENTS

We acknowledge financial support from the Fundamental Research Funds for the Central Universities (No. 2018QJ06) and the National Basic Research Program of China (973 Program, No. 2015CB352100).

References

1. M. Pule, A. Yahya and J. Chuma, *J. Appl. Res. Technol.*, 15(2018) 562.
2. Y. Chen and D. Han, *Automat. Constr.*, 89(2018) 307.
3. R. Martínez-Mañez, J. Soto, J. Lizondo-Sabater, E. García-Breijo, L. Gil, J. Ibáñez and I. Alcaina, S. Alvarez, *Sens. Actuators, B*, 101 (2004) 295.
4. S. Zhuiykov and K. Kalantar-zadeh, *Electrochim. Acta*, 73 (2012) 105.
5. L. Cui, J. Wu and H. Ju, *Biosens. Bioelectron.*, 63(2015) 276.
6. A. B. Chimezie, R. Hajian, N. A. Yusof, P. M. Woi and N. Shams, *J. Electroanal. Chem.*, 796(2017) 33.
7. E. Silva, A.C. Bastos, M. Neto, A. Fernandes, R. Silva, M. Ferreira, M. Zheludkevich and F. Oliveira, *Sens. Actuators, B*, 204 (2014) 544.
8. A. Rahim, L. Santos, S. Barros, L. Kubota and Y. Gushikem, *Sens. Actuators, B*, 177 (2013) 231.
9. S. Wu, Q. He, C. Tan, Y. Wang and H. Zhang, *Small*, 8 (2013) 1160.
10. E. B. Bahadır and M. K. Sezgintürk, *Trends Anal. Chem.*, 76(2016) 1.
11. L. Wang, E. Hua, M. Liang, C. Ma, Z. Liu, S. Sheng, M. Liu, G. Xie and W. Feng, *Biosens. Bioelectron.*, 51 (2014) 201.
12. P. Lee, Z. Wang, X. Liu, Z. Chen and E. Liu, *Thin Solid Films*, 584 (2015) 85.
13. F. Bai, H. Huang, Y. Tan, C. Hou and P. Zhang, *Electrochim. Acta*, 176 (2015) 280.
14. E. Bayram, G. Yilmaz and S. Mukerjee. *Appl. Catal., B: Environ.*, 192 (2016) 26.
15. X. Qiu, L. Lu, J. Leng, Y. Yu, W. Wang, M. Jiang and L. Bai, *Food Chem.*, 190 (2016) 889.
16. E. Er, H. Çelikkan, N. Erk and M. Aksu, *Electrochim. Acta*, 157 (2015) 252.
17. M. Pumera, *Electrochem. Commun.*, 36 (2013) 14.
18. L. Yang, D. Liu, J. Huang and T. You, *Sens. Actuators, B*, 193 (2014) 166.
19. H. Filik, G. Çetintaş, A. Avan, S. Aydar, S. Koç and İ. Boz, *Talanta*, 116 (2013) 245.
20. X. Hu, W. Dou and G. Zhao, *J. Electroanal. Chem.*, 756 (2015) 43.
21. A. Wong, C. Razzino, T. Silva and O. Fatibello-Filho, *Sens. Actuators, B*, 231 (2016) 183.
22. H. Ma, J. Sun, Y. Zhang, C. Bian, S. Xia and T. Zhen, *Biosens. Bioelectron.*, 80 (2016) 222.
23. M. Hilder, B. Winther-Jensen, D. Li, M. Forsyth and D. MacFarlane, *Phys. Chem. Chem. Phys.*, 13 (2011) 9187.
24. Y. Li, J. Sun, J. Wang, C. Bian, J. Tong, Y. Li and S. Xia, *Biochem. Eng. J.*, 123 (2017) 86.
25. X. Hu, W. Dou and G. Zhao, *J. Electroanal. Chem.*, 756 (2015) 43.
26. F. Shi, J. Xi, F. Hou, L. Han, G. Li, S. Gong, C. Chen and W. Sun, *Mater. Sci. Eng., C*, 58 (2016) 450.
27. B. Li, L. Zhou, D. Wu, H. L. Peng, K. Yan, Y. Zhou and Z. F. Liu, *ACS Nano*, 5 (2011) 5957.
28. J. Wang, C. Bian, J. Tong, J. Sun, Y. Li, W. Hong and S. Xia, *Sensors*, 15 (2014) 382.
29. I. Tiwari, M. Gupta, R. Prakash and C. E. Banks, *Analytical Methods*, 6 (2014) 8793.
30. L. Liu, J. Zhai, C. Zhu, Y. Gao, Y. Wang, Y. Han and S. Dong, *Biosens. Bioelectron.*, 63 (2015) 483.

31. S. Rastogi, A. Kumar, N.K. Mehra, S.D. Makhijani, A. Manoharan, V. Gangal and R. Kumar, *Biosens. Bioelectron.*, 18 (2003) 23.
32. K.B. Hooi, A.K. Ismail, R. Ahamad and S. Shahir, *Electrochim. Acta*, 176 (2015) 777.

© 2018 The Authors. Published by ESG (www.electrochemsci.org). This article is an open access article distributed under the terms and conditions of the Creative Commons Attribution license (<http://creativecommons.org/licenses/by/4.0/>).